16TH EUROPEAN CONFERENCE ON EARTHQUAKE ENGINEERING THESSALONIKI 18 - 21 JUNE 2018

PERFORMANCE BASED OPTIMAL SEISMIC RETROFITTING WITH NONLINEAR FLUID VISCOUS DAMPERS IN THE PRESENCE OF YIELDING

Nicolò POLLINI[1], Oren LAVAN[2], Oded AMIR[3]

ABSTRACT

We present a new methodology for achieving economical retrofitting design solutions of frames with nonlinear hysteretic behavior. Nonlinear fluid viscous dampers and their supporting braces are distributed and sized with an optimization-based approach. In order to identify design solutions useful for practitioners, a realistic retrofitting cost function is minimized. The inter-story drifts are constrained to allowable values. These are evaluated with nonlinear time-history analyses considering realistic ground acceleration records. The behavior of each damper-brace system is defined based on the Maxwell's model for viscoelasticity. A fractional power-law is used to describe the nonlinear force-velocity relation of each damper, and the stiffening contribution of the supporting brace and of the damper is modeled by linear springs. The structure is modeled with a mixed finite element approach, where the hysteretic behavior is defined at the elements' sections level. Moreover, the proposed approach accounts for the interaction in the structural elements between axial force and bending moment. The damper-brace elements are divided into size-groups, that is, elements with the same mechanical properties. The properties of each size-group of dampers, and the dampers' distribution in the structure are optimally defined using Genetic Algorithms. The ability of the proposed approach to identify economical designs is demonstrated in a practical case. The numerical results establish also important benchmarks for other, more efficient, methods to be developed.
Keywords: nonlinear fluid viscous dampers; Maxwell model; hysteretic frames; nonlinear time-history analysis; genetic algorithm.

1. INTRODUCTION

There are structures whose behavior can not be expected to be linear in the eventuality of severe seismic events, even if a reasonable amount of damping is added to the structure. In this category could be included for example irregular structures and tall buildings. In some cases, the behavior of certain tall buildings may remain in the elastic range even without using additional viscous dampers. Nevertheless, if dampers are added, axial forces in the columns at the lower stories may reach their yielding limits. Thus, in these cases the nonlinearity of the structural behavior should be accounted for, to properly consider this effect. The use of linear analysis tools may fail to give a good estimate of the structural response in these cases. Hence, nonlinear analysis tools are required. Nonlinear analysis tool are also needed when a more detailed study of the structural response due to the coupling of an added damping system is required.

Methodologies have been proposed for the distribution and sizing of fluid viscous dampers based on optimization. Several authors proposed methodologies for the general optimization problem of the simultaneous dampers' distribution and size selection (Dargush & Sant, 2005; Lavan & Dargush, 2009; Kanno, 2013; Gluck, Reinhorn, Gluck, & Levy, 1996; Singh & Moreschi, 2002; Lavan & Levy, 2006; Lavan & Amir, 2014). Some authors focused on the retrofitting of nonlinear structures with linear dampers (Lavan & Levy, 2005; Lavan & Levy, 2010; Lavan, 2015). More recently, in (Gidaris &

[1]Postdoc, Faculty of Mechanical Engineering, Technical University of Denmark, Lyngby, Denmark, nipol@mek.dtu.dk
[2]Associate Professor, Faculty of Civil and Environmental Engineering, Technion – Israel Institute of Technology, Haifa, Israel, lavan@technion.ac.il
[3]Assistant Professor, Faculty of Civil and Environmental Engineering, Technion – Israel Institute of Technology, Haifa, Israel, odedamir@technion.ac.il

Taflanidis, 2015) an optimization-based approach for the minimization of the life-cycle cost for nonlinear structures with nonlinear dampers was discussed. There, a probabilistic approach was adopted for estimating the life-cycle cost, and a stochastic approach was used to optimize the systems considered. However, the dampers were modeled as pure dashpots, disregarding any stiffening contribution of the supporting braces and of the dampers.

In general, dampers are connected to the structure and to a supporting brace, and often, the assumption of 'infinitely stiff' braces is made. As a matter of fact, braces have an upper limit in terms of their stiffness. Considering a finite stiffness of the brace could significantly affect the damper-brace mechanical behavior (Akcelyan, Lignos, Hikino, & Nakashima, 2016). In recent work, a nonlinear behavior of the viscous dampers was considered (Dall'Asta, Scozzese, Ragni, & Tubaldi, 2017; Tubaldi, Barbato, & Dall'Asta, 2014; Tubaldi, Ragni, & Dall'Asta, 2015), including also in some cases the stiffening effect of the supporting braces and the dampers (Pollini, Lavan, & Amir, 2017; Pollini, Lavan, & Amir, 2017). The results discussed in this paper constitute an additional contribution to the retrofitting problem of nonlinear structures with nonlinear fluid viscous dampers, through a practical and effective optimization-based approach. In fact, from a computational point of view it represents the most demanding type of seismic retrofitting problem, due to its nonlinearity. The coupling between the structure and the added damping system require more sophisticated analysis tools. Additionally, large scale structures are characterized by large numbers of design variables such as those related to the dampers' size and placement in the structure.

Herein, we will consider damper-brace elements made of two linear springs and a nonlinear dashpot in series. Thus, it will be possible to account for the stiffness of the braces and of the dampers, and for the damping property of the viscous dampers. As in the previous application, here too the realistic retrofitting cost presented in (Pollini, Lavan, & Amir, 2017) is minimized. The dampers and their supporting braces are distributed in given structures and sized, selecting their sizes from a limited set of available size-groups. Each size-group is characterized by damper-brace elements with the same mechanical properties. The size-groups are limited in number to achieve final practical designs, but their properties are not predefined and are optimized simultaneously within a single problem formulation. Inter-story drifts are constrained to allowable values. These are evaluated with nonlinear time-history analyses considering realistic ground motions. The structure is modeled with a mixed finite element approach, where the hysteretic behavior is defined at the elements' sections level. Moreover, the proposed approach accounts for the interaction in the structural elements between axial force and bending moment. The problem is formulated as a mixed-integer optimization problem, and it is solved with Genetic Algorithms (GA).

2. Governing Equations

In the following section, we first present the model considered for the definition of the damper-brace behavior and the relative equations. Then, we recall the equations of motion for a structure with nonlinear behavior and equipped with nonlinear fluid viscous dampers, and subject to a realistic ground motion acceleration.

2.1 Damper-brace system characterization

In this work, we consider damper-brace systems made of two springs and a dashpot in series, as shown in Figure 1, (Oohara & Kasai, 2002).

Figure 1 Stiffening and damping contributes of the damper-brace system

The first spring accounts for the stiffness of the supporting brace, while the second for the stiffness of the damper. Last, the dashpot accounts for the damping property of each damper. The two springs are

modeled with a linear force-displacement behavior, while a fractional power law defines the dashpot force-velocity behavior:

$$\begin{aligned} f_b &= k_b u_b \\ f_d &= k_d u_d \\ f_d &= c_d \text{sign}(\dot{u}_d)|\dot{u}_d|^{\alpha} \end{aligned} \quad (1)$$

where f_b is the force in the brace, and f_d is the force in the damper; k_b is the brace stiffness, k_d the damper stiffness, and c_d its damping coefficient; u_b is the elongation of the brace, u_d the elongation of the damper, and $\dot{u}_d$ the relative velocity between the ends of the damper. The exponent $0 < \alpha \leq 1$ characterizes the nonlinear behavior of the dashpot. For α equal to one the damper is linear, while for α that tends to zero the formulation mimics the behavior of a friction damper. The exponent α significantly affects the computational effort required for integrating the equations of motion. The algorithm for the time-history analysis developed by the authors and used in this work successfully solved the equations of motion for values of α between 0.1 and 1. Herein we will consider α equal to 0.35, as in (Akçelyan & Lignos, 2015). Because of equilibrium, the forces in the damper and in the brace are equal ($f_b = f_d$). It follows that:

$$k_b u_b = k_d u_d = c_d \text{sign}(\dot{u}_d)|\dot{u}_d|^{\alpha} \quad (2)$$

The axial stiffness of a brace can be easily calculated. The stiffness contribution of a fluid viscous damper, on the contrary, is far less intuitive. It depends in fact on:

1. The stiffness of the metal parts of the damper from one end to the other;
2. The stiffness of the fluid column inside the damper;
3. The expansion of the damper cylinder under pressure (which makes the fluid seem more compressible).

Among the three components mentioned above, the second is the more complex to be defined. The fluid under pressure behaves according to its bulk modulus curve, which is nonlinear. However, dampers of a single manufacturer typically have their peak forces at similar limit pressures, and in general they are also made of the same materials. Thanks to this, many of the variables drop out. As a result, the end to end stiffness of a fluid viscous damper, as tested by Taylor Devices (Taylor, 2015), is such that it will reach its rated force at approximately 3% of its rated stroke from the centered position. This defines the stiffness of the damper that can be considered as a constant property of the device.

The ratio between the damping coefficient of a damper and the stiffness of the damper and the brace is very important in the solution of the equations of motion. In fact, it affects the computational effort and the complexity of the integration technique required in each time step. This is particularly true in the case of nonlinear fluid viscous dampers. For this reason, we define a priori the ratio between the damping coefficient of the damper and the equivalent stiffness resulting from the brace and the damper, as discussed in (Pollini, Lavan, & Amir, 2017).

Once the ratio ρ is defined, we can express k_{eq} as:

$$k_{eq} = \rho c_d \quad (3)$$

Therefore, for each damper-brace element the damping coefficient c_d is the design variable, for a given ratio ρ and exponent α (Figure 2).

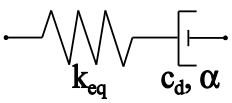

Figure 2 Equivalent Maxwell's model for the brace-damper system

2.2 Equations of motion

We consider generic planar frames subject to a realistic ground motion. The structures are modeled with beam finite element with nonlinear hysteretic behavior. The nonlinear behavior is defined at the element

sections level in terms of a hysteretic moment curvature relation (i.e. M-χ) as in (Sivaselvan & Reinhorn, 2000). Nonlinear damper-brace elements are distributed in predefined potential locations of the structure. They all share the same ratio ρ, and exponent α, that have been already presented in Sec. 2.1. Each damper is characterized by a specific damping coefficient c_d. The responses of interest are evaluated with nonlinear time-history analyses. In each time-step, the yielding moment of each element is updated based on the element axial force calculated at the previous time-step. For each point *t* in time, the dynamic behavior of a structure with N_{dof} degrees of freedom and N_d potential location for dampers is defined by the following set of equations of motion:

$$\begin{aligned} &\mathbf{M}\ddot{\mathbf{u}}(t)+\mathbf{C}_s\dot{\mathbf{u}}(t)+\mathbf{F}_s(t)+\mathbf{T}_d{}^T\mathbf{f}_d(t)=-\mathbf{M}\mathbf{e}a_g(t) \\ &\dot{\mathbf{f}}_d(t)=D(\mathbf{k}_{eq})\left[\mathbf{T}\dot{\mathbf{u}}(t)\sin(\beta)-\left(D(\mathbf{c}_d)^{-1}D(|\mathbf{f}_d(t)|)\right)^{\frac{1}{\alpha}}\operatorname{sign}(\mathbf{f}_d(t))\right] \end{aligned} \tag{4}$$

In Eq. (4): $\mathbf{M}$ is the mass matrix; $\mathbf{C}_s$ is the inherent damping matrix; $\mathbf{u}(t)$ is the displacement vector of the degrees of freedom; $\mathbf{f}_d(t)$ is the vector of the resisting forces of the dampers; $\mathbf{F}_s(t)$ is the vector of the resisting forces of the structure; $\mathbf{e}$ is the location vector that defines the location of the excitation; and $a_g(t)$ is the ground acceleration. $D(\cdot)$ is an operator that transforms a vector into a diagonal matrix, and a diagonal matrix into a vector (as the *diag* MATLAB function does). The matrix $\mathbf{T}_d$ is a transformation matrix, that transforms the global coordinates for the displacements and velocities ($\mathbf{u}$, $\dot{\mathbf{u}}$) into local coordinates ($\mathbf{d}$, $\dot{\mathbf{d}}$), namely inter-story drifts and velocities.

In order to be solved, the problem is first discretized in time, and then solved with the Newmark-β method. In particular, in each time step the equilibrium is achieved by means of an iterative procedure. In this procedure, in each step the dampers' forces are approximated with a fourth-order explicit Runge-Kutta method, as suggested in (Oohara & Kasai, 2002; Pollini, Lavan, & Amir, 2017). For more details on Runge-Kutta methods please refer to (Quarteroni, Sacco, & Saleri, 2010). The structural response is then corrected with the Newton-Raphson method (Spacone, Ciampi, & Filippou, 1992). The iterative procedure stops when the residual forces are sufficiently small.

3. Optimization problem formulation

In this paper, we formulate and solve the problem for the optimal distribution and sizing of nonlinear fluid viscous dampers. A realistic retrofitting cost function is minimized while selected structural performance indices are limited to maximum allowable values. The dampers are chosen from two available size-groups, and distributed in potential locations of a given structure. The properties of each size-group are also optimized and not predefined. Thus, in this section we present the design variables involved in the problem formulation, the new retrofitting cost function, and the constrained performance indexes.

3.1 Design variables

The goal is to size and distribute up to N_d nonlinear fluid viscous dampers in predefined potential locations of a given frame. They can be chosen out of two available size-groups, where for size-group we intend a group of dampers with the same characteristics. In each location, we allow the algorithm to distribute as many as two damper. Therefore, we have to determine $2N_d$ damping coefficients c_{di}, that are collected in the vector $\mathbf{c}_d$. The vector of damping coefficients is defined as follows:

$$\mathbf{c}_d=\bar{c}_d D(\mathbf{x}_1)\left(y_1\mathbf{1}+(y_2-y_1)\mathbf{x}_2\right) \tag{5}$$

In Eq. (5): $D()$ is the diagonal operator which transforms a vector into a diagonal matrix; $\mathbf{1}$ is the unit vector; $\bar{c}_d$ represents the maximum damping coefficient available, and it is defined a priori. The vector $\mathbf{x}_1$ has binary entries representing the existence of a damper in each potential locations. In particular, a value of zero in the *i*-th entry of the vector will mean that in the location *i* there is no damper, while a value of one that there is a damper. Also $\mathbf{x}_2$ is a vector with binary entries, representing the association

of each existing damper to one of the two available size-groups. In the case of x_{2i} equal to zero, the damper in the *i*-th location belongs to the first size-group. In the case of x_{2i} equal to one, the damper in the *i*-th location belongs to the second size-group. We should also mention that the dimensions of the vectors $\mathbf{c}_d$, $\mathbf{x}_1$, and $\mathbf{x}_2$ are $2N_d \times 1$. The two available damping coefficients that define the two size-groups are:

$$c_{d1}=\bar{c}_d y_1, \quad c_{d2}=\bar{c}_d y_2 \tag{6}$$

In Eq. (6), y_1 and y_2 are two continuous design variables that scale the maximum available damping coefficient $\bar{c}_d$. Last, it should be noted that the design indirectly extends also to the dampers' supporting braces through the parameter ρ, as it has already been illustrated in Sec. 2.1.

3.2 Cost function

One of the main contributions of the present work consists in minimizing a realistic retrofitting cost function. The cost function is inspired by the one presented in (Pollini, Lavan, & Amir, 2017). Therefore, also in this case the cost function J consists of three cost components:

$$J=J_l+J_m+J_p \tag{7}$$

The first cost component J_l represents the cost associated with the number of locations in which dampers are installed. We allow the algorithm to allocate as many as two dampers in each potential location; hence, this component includes all costs associated with the preparation of the structure for the damper installation and the architectural constraint that this installation will represent. Moreover, in case of retrofitting, it can also account for the removal of existing nonstructural components. The first component of the cost is defined as follows:

$$J_l=\mathbf{C}_l^T\mathbf{x}_1 \tag{8}$$

where $\mathbf{C}_l$ is a $2N_d \times 1$ vector in which the *i*-th component is a cost component related to the *i*-th component of $\mathbf{x}_1$. The vector $\mathbf{C}_l$ is the sum of two components that account for the costs of placing the first (i.e. $\mathbf{C}_{l1}$) and second (i.e. $\mathbf{C}_{l2}$) damper in each potential location as in (Pollini, Lavan, & Amir, 2016).

The second cost component, J_m, represents the manufacturing cost of the dampers. In principle, the manufacturing cost of viscous dampers depends on the peak stroke and on the square root of the peak force of the most loaded damper of each size-groups. We assume, in fact, that all dampers of a specific size-group are designed so to have the same capacity. Since we are constraining inter-story drifts, also the peak stroke of the dampers is indirectly limited. As a consequence, it does not affect significantly the cost. Therefore, the manufacturing cost is defined as the square root of the peak force of the most loaded damper from each size-group, multiplied by the number of dampers of each size-group. Formally, it is written as follows:

$$J_m=C_m\left\{\mathbf{x}_1^T(\mathbf{1}-\mathbf{x}_2)\left[\max(\hat{\mathbf{f}}_{d1})\right]^{0.5}+\mathbf{x}_1^T\mathbf{x}_2\left[\max(\hat{\mathbf{f}}_{d2})\right]^{0.5}\right\} \tag{9}$$

where C_m is a scalar cost component which gives the desired proportion between J_m and the other cost components, and:

$$\begin{aligned}\hat{\mathbf{f}}_{d1}&=D(\mathbf{1}-\mathbf{x}_2)\hat{\mathbf{f}}_d\\ \hat{\mathbf{f}}_{d2}&=D(\mathbf{x}_2)\hat{\mathbf{f}}_d\\ \hat{\mathbf{f}}_d&=\max_t(|\mathbf{f}_d(t)|)\end{aligned} \tag{10}$$

$\hat{\mathbf{f}}_d$ is the vector of the peak forces in time for all dampers; the vector $\hat{\mathbf{f}}_{d1}$ has the components of $\hat{\mathbf{f}}_d$ which belongs to dampers of the first size-group, while $\hat{\mathbf{f}}_{d2}$ those of the second size-group. It should be noted

that the *max* function in Eq. (9) refers to the components of the vectors $\hat{\mathbf{f}}_{d1}$ and $\hat{\mathbf{f}}_{d2}$, and the result is a scalar. On the contrary, in Eq. (10) the *max* function refers to the maximum absolute value in time for each component of the vector $\mathbf{f}_d(t)$, and the result is a vector.

Modern seismic codes require to test one damper prototype for each size-group so to verify its force-velocity behavior. As a results, we consider an additional cost component, J_p. This component is formulated so that the number of different size-groups of dampers used for retrofitting should be minimized:

$$J_p=C_p\left[H\left(\mathbf{x}_1^T\mathbf{x}_2\right)+H(\mathbf{x}_1^T(\mathbf{1}\text{-}\mathbf{x}_2))\right] \tag{11}$$

where C_p is the cost of prototype testing and design. The function H is the Heaviside step function:

$$H(x)=\begin{cases}1 \text{ for } x>0\\ 0 \text{ for } x=0\end{cases} \tag{12}$$

We observe that:

- If all dampers are of the first size then J_p will be equal to $C_p \times [0+1]$;
- If all dampers are of the second size then J_p will be equal to $C_p \times [1+0]$;
- In case dampers of both size exist then J_p will be equal to $C_p \times [1+1]$.

3.3 Performance index

We are now considering the seismic retrofitting of hysteretic frames using nonlinear fluid viscous dampers. As in (Pollini, Lavan, & Amir, 2017), here too inter-story drifts are used as an appropriate measure of both structural and nonstructural damage levels. Moreover, by limiting the inter-story drifts it is possible to constrain the response of the structure to a linear behavior. This can be done by limiting the inter-story drifts to the value of drift for which yielding occurs. In particular, the peak inter-story drift normalized by the allowable value is chosen as the local performance index for 2-D frames:

$$d_{ci}=\max_t\left(\left|d_i(t)/d_{allow,i}\right|\right)\leq 1 \quad \forall\, i=1,\ldots,N_{drifts} \tag{13}$$

where $d_i(t)$ is the inter-story drift *i* at time t; $d_{allow,i}$ its maximum allowable value; and N_{drifts} is the number of drifts to be constrained.

3.4 Mixed-integer optimization problem

At this point, we presented all the ingredients of our optimization problem. The following is its mixed-integer formulation:

$$\begin{aligned}
&\min_{\mathbf{x}_1,\mathbf{x}_2,y_1,y_2} \quad J=J_l+J_m+J_p\\
&\text{s.t.: } d_{c,i}=\max_t\left(\left|d_i(t)/d_{allow,i}\right|\right)\leq 1 \;\forall i=1,\ldots,N_{drifts}\\
&x_{1,k}=\{0,1\} \text{ for } k=1,\ldots,2N_d\\
&x_{2,k}=\{0,1\} \text{ for } k=1,\ldots,2N_d\\
&0 \leq y_1 < y_2 \leq 1\\
&\text{with: } \mathbf{M}\ddot{\mathbf{u}}(t)+\mathbf{C}_s\dot{\mathbf{u}}(t)+\mathbf{F}_s(t)+\mathbf{T}_d^T\mathbf{f}_d(t)=-\mathbf{M}\mathbf{e}a_g(t)\\
&\dot{\mathbf{f}}_d(t)=D\left(\mathbf{k}_{eq}\right)\left[T\dot{\mathbf{u}}(t)\sin(\beta)-\left(D(\mathbf{c}_d)^{-1}D(|\mathbf{f}_d(t)|)\right)^{\frac{1}{\alpha}}\operatorname{sign}\left(\mathbf{f}_d(t)\right)\right]\\
&\mathbf{u}(0)=u_0,\ \dot{\mathbf{u}}(0)=\dot{u}_0,\ \mathbf{F}_s(0)=\mathbf{F}_{s0},\ \mathbf{f}_d(0)=\mathbf{f}_{d0}
\end{aligned} \tag{14}$$

For optimizing the distribution and size of a single damper size-group, only the $\mathbf{x}_1$ and y_1 variables are necessary, thus it can be seen as a particular case of the two-damper size-group optimization. The problem (14) has been solved with a GA. The results will be presented in Sec. 4.

4. NUMERICAL EXAMPLE

In the following section, we present and discuss a numerical application. The results have been obtained by optimizing a realistic plane frame. It should be noted that, even though the numerical results refer to a 2D frame, the approach presented herein could be extended to the case of 3D structures with no particular additional modifications. The mixed-integer problem formulation presented previously has been solved using MATLAB's built-in GA. In particular, we consider the north-south moment resisting frame of a nine-story benchmark building presented in (Ohtori, Christenson, Spencer, & Dyke, 2004). The details of the frame can be found in (Ohtori, Christenson, Spencer, & Dyke, 2004). For this example, the coefficient ρ of the damper-brace elements was defined according to the procedure presented in (Pollini, Lavan, & Amir, 2017). However, after numerical tests it was noticed that assigning the same parameter ρ to all the dampers did not give the desired results. The dampers of higher stories tended to behave more as spring element due to the participation of higher modes in the vibration of the higher stories. For this reason, we modified the procedure discussed (Pollini, Lavan, & Amir, 2017), and we considered in the tuning procedure the first three modes of vibration of the structure. In particular, we considered ω_1 for the dampers in locations 1-3, ω_2 for the dampers in locations 4-6, and ω_3 for the dampers in locations 7-9. Additionally, since the stories had different heights they were also subjected to different values of allowable inter-story drifts. Thus, we assigned to the damper-brace elements four different values of the parameters ρ depending on their location in the structure. With respect to the scheme of Figure 4, the parameters ρ are assigned as in Table 1 .

Table 1 Values of the parameters ρ assigned to the dampers

Damper location	1	2	3	4	5	6	7	8	9
Value of ρ	ρ_1	ρ_2	ρ_2	ρ_3	ρ_3	ρ_3	ρ_4	ρ_4	ρ_4

In Table 1, ρ_1=0.5690, ρ_2=0.5194, ρ_3=0.8838, and ρ_4=1.1389. Regarding the ground motion acceleration, out of the ensemble LA 10% in 50 years (National Information Service for Earthquake Engineering , 2013), LA05 was considered acting in the horizontal direction since it proved to cause the largest inter-story drift in the frame without dampers. The ground acceleration record considered is plotted in Figure 3.

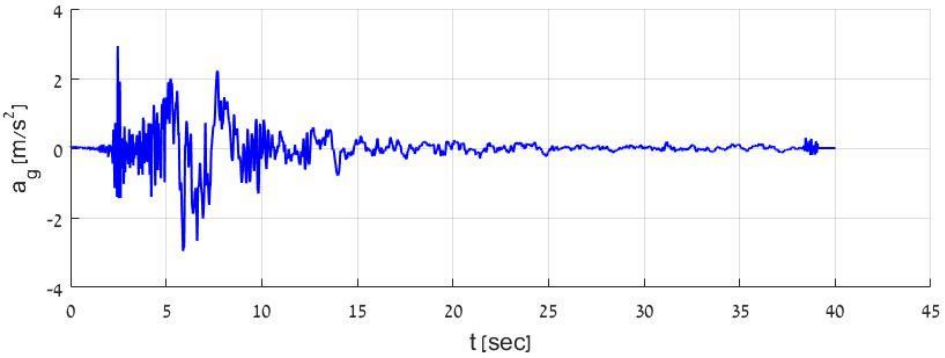

Figure 3 LA05 ground acceleration record, from the ensemble LA 10% in 50 years

In this example, we considered 5% of critical damping for the first and the fifth modes in order to build the Rayleigh damping matrix of the structures. In Table 2 the numerical values of several parameters involved in the problem formulation are presented. It should be noted that the cost components different from zero of the vector $\mathbf{C}_{l1}$, and $\mathbf{C}_{l2}$ were all equal in the numerical experiments.

Table 2 Values of the parameters used in the numerical examples. h is the story height

Parameter	d_{allow} [as h]	$\bar{c}_d$ [kN(s/mm)$^{\alpha}$]	α [#]	C_{l1} [#]	C_{l2} [#]	C_m [1/kN$^{0.5}$]	C_p [#]
Value	h/100	500	0.35	100	50	1	50

In the GA implementation, the population size was set to 350. In order to guarantee the convergence of the algorithm to a global optimum with high probability, five different analyses were performed, of which the best solution was chosen. In this case we defined two criteria for convergence: The first halts the algorithm when the number of generations (i.e. iterations) reaches the maximum number allowable `Generations` - 500; The second halts the algorithm when the weighted average relative change in the best fitness function value over `StallGenLimit` generations is less than or equal to `TolFun`. `StallGenLimit` is an integer set to 50, and `TolFun` is a positive scalar set to 10^{-6}.

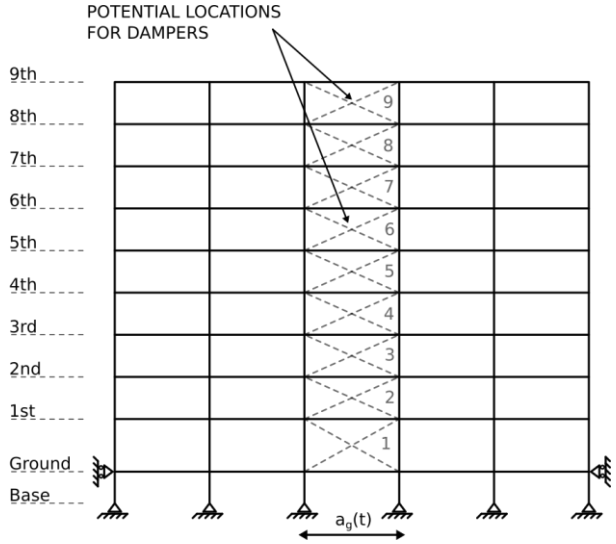

Figure 4 Potential locations for dampers in the nine-story moment resisting frame.

With GA, the analysis that led to the best solution converged after 73 iterations (approximately 4 days for the single GA analysis using 12 CPUs on a computer cluster hosted and maintained by the Division for Computing and Information Systems at the Technion - Israel Institute of Technology), leading to a final distribution of dampers characterized by only one damping coefficient: $\bar{c}_2$ =497.49 [kN(s/mm)$^{\alpha}$], and a final cost J=923.04. The optimized distribution and damper sizes obtained is shown in Figure 6. In Figure 5 we show the response of the structure with the optimized distribution of dampers in terms of inter-story drift versus time. In particular, we show the response of the second inter-story drift (i.e. $d_2(t)$) since it has the largest peak value in time compared to the other drifts constrained, and it reaches the maximum allowable value.

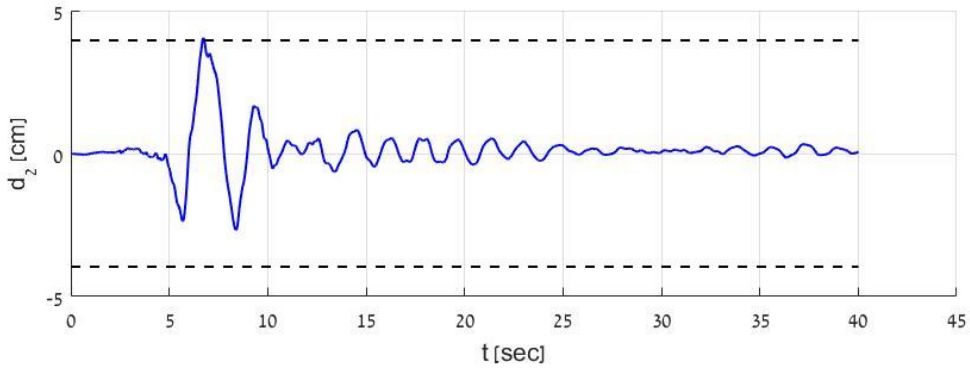

Figure 5 Response of the second inter-story drift (i.e. $d_2(t)$) of the structure with the optimized distribution of dampers. The dashed line represents the maximum allowable value of the drift at location 2 (i.e. 3.96 cm)

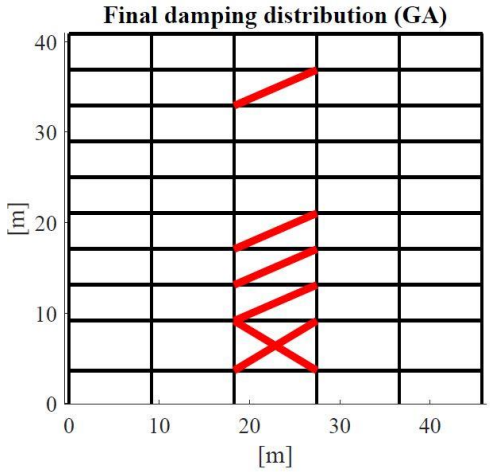

Figure 6 Final damping distribution having 9 potential locations for dampers. Locations 1, 2, 3, 4, and 8 are actually occupied by dampers in the final solution. Only one size-group of dampers is actually present in the solution: $\bar{c}_2$ =497.49 [kN(s/mm)$^{\alpha}$]

5. CONCLUSIONS

In this paper we presented a novel, effective formulation for the minimum-cost seismic retrofitting of hysteretic nonlinear structures with nonlinear fluid viscous dampers. The objective function of the optimization problem is the retrofitting cost function, and it is made of three components: The cost associated with the installation of a damper in a specific location in the frame; The manufacturing cost of the dampers; The cost of prototype design and testing. The dampers are modelled with a nonlinear force-velocity behavior defined by a fractional power law. Their interaction with the supporting members and the structure is accounted based on the Maxwell's model for viscoelasticity. The inter-story drifts are evaluated with nonlinear time-history, and constrained to an allowable value. The structure is modeled with a mixed finite element approach, where the hysteretic behavior is defined at the elements' sections level. In the proposed approach we account also for the interaction in the structural elements between axial force and bending moment.

Main contribution of the present work is the new optimization problem formulation, that addresses the seismic retrofitting of nonlinear structures with nonlinear fluid viscous. As a result, we can provide practitioners with an effective performance-based design tool for the seismic retrofitting of generic structures subject to realistic ground motions. The results presented herein show the effectiveness of the presented approach in a realistic design case. In particular, in the example the algorithm identified minimum cost design solutions for the given structural performance limitations. Additionally, the work presented in this paper, including the nonlinear damper-brace model, the problem formulation and the results attained, provide an important foundation for further developments on the subject. These will focus on increasing the computational efficiency by solving the problem with a gradient-based optimization approach.

6. ACKNOWLEDGMENTS

The research presented in this paper was founded by the Israeli Ministry of Science, Technology and Space. The authors gratefully acknowledge this financial support.

7. REFERENCES

Akçelyan, S., & Lignos, D. G. (2015). *Dynamic Analyses of 1-Story Moment Frame with Viscous Dampers*. Retrieved from OpenSeesWiki.

Akcelyan, S., Lignos, D. G., Hikino, T., & Nakashima, M. (2016). Evaluation of simplified and state-of-the-art analysis procedures for steel frame buildings equipped with supplemental damping

devices based on E-Defense full-scale shake table tests. *Journal of Structural Engineering*.
Dall'Asta, A., Scozzese, F., Ragni, L., & Tubaldi, E. (2017). Effect of the damper property variability on the seismic reliability of linear systems equipped with viscous dampers. *Bulletin of Earthquake Engineering*.
Dargush, G. F., & Sant, R. S. (2005). Evolutionary aseismic design and retrofit of structures with passive energy dissipation. *Earthquake Engineering and Structural Dynamics, 34*, 1601-1626.
Gidaris, I., & Taflanidis, A. A. (2015). Performance assessment and optimization of fluid viscous dampers through lifecycle. *Bulletin of Earthquake Engineering*.
Gluck, N., Reinhorn, A. M., Gluck, J., & Levy, R. (1996). Design of supplemental dampers for control of structures. *Journal of Structural Engineering*.
Kanno, Y. (2013). Damper placement optimization in a shear building model with discrete design variables: a mixed-integer second-order cone programming approach. *Earthquake Engineering & Structural Dynamics, 42*(11), 1657-1676.
Lavan, O. (2015). A methodology for the integrated seismic design of nonlinear buildings with supplemental damping. *Structural Control and Health Monitoring*.
Lavan, O., & Amir, O. (2014). Simultaneous topology and sizing optimization of viscous dampers in seismic retrofitting of 3D irregular frame structures. *Earthquake Engineering & Structural Dynamics, 43*(9), 1325-1342.
Lavan, O., & Dargush, G. F. (2009). Multi-objective evolutionary seismic design with passive energy dissipation systems. *Journal of Earthquake Engineering, 13*, 758-790.
Lavan, O., & Levy, R. (2005). Optimal design of supplemental viscous dampers for irregular shear-frames in the presence of yielding. *Earthquake Engineering & Structural Dynamics, 34*(8), 889-907.
Lavan, O., & Levy, R. (2006). Optimal design of supplemental viscous dampers for linear framed structures. *Earthquake Engineering & Structural Dynamics*.
Lavan, O., & Levy, R. (2010). Performance based optimal seismic retrofitting of yielding plane frames using added viscous damping. *Earthquake and Structures*.
National Information Service for Earthquake Engineering . (2013). *10 pairs of horizontal ground motions for Los Angeles with a probability of exceedence of 10% in 50 years.* University of California, Berkeley.
Ohtori, Y., Christenson, R. E., Spencer, B. F., & Dyke, S. J. (2004). Benchmark control problems for seismically excited nonlinear buildings. *Journal of Engineering Mechanics*.
Oohara, K., & Kasai, K. (2002). Time-history analysis model for nonlinear viscous dampers. *Structural Engineers World Congress (SEWC).* Yokohama, Japan.
Pollini, N., Lavan, O., & Amir, O. (2016). Towards realistic minimum-cost optimization of viscous dampers for seismic retrofitting. *Bulletin of Earthquake Engineering, 14*(3), 1-28.
Pollini, N., Lavan, O., & Amir, O. (2017). Adjoint sensitivity analysis and optimization of hysteretic dynamic systems with nonlinear viscous dampers. *Structural and Multidisciplinary Optimization*.
Pollini, N., Lavan, O., & Amir, O. (2017). Minimum-cost optimization of nonlinear fluid viscous dampers and their supporting members for seismic retrofitting. *Earthquake Engineering & Structural Dynamics*.
Quarteroni, A., Sacco, R., & Saleri, F. (2010). *Numerical mathematics (Vol. 37).* Springer Science & Business Media.
Singh, M. P., & Moreschi, L. M. (2002). Optimal placement of dampers for passive response control. *Earthquake Engineering & Structural Dynamics*.
Sivaselvan, M. V., & Reinhorn, A. M. (2000). Hysteretic models for deteriorating inelastic structures. *Journal of Engineering Mechanics*.
Spacone, E., Ciampi, V., & Filippou, F. C. (1992). *A beam element for seismic damage analysis.* Berkeley: Earthquake Engineering Research Center, College of Engineering, University of California at Berkeley.
Taylor, D. (2015). Personal communication.
Tubaldi, E., Barbato, M., & Dall'Asta, A. (2014). Performance-based seismic risk assessment for buildings equipped with linear and nonlinear viscous dampers. *Engineering Structures*.
Tubaldi, E., Ragni, L., & Dall'Asta, A. (2015). Probabilistic seismic response assessment of linear

systems equipped with nonlinear viscous dampers. *Earthquake Engineering & Structural Dynamics*.